Pan-transcriptome-based candidate therapeutic discovery for idiopathic pulmonary fibrosis

Yunguan Wang, Jaswanth K. Yella, Sudhir Ghandikota, Tejaswini C. Cherukuri, Harshavardhana H. Ediga, Satish K. Madala and Anil G. Jegga

Ther Adv Respir Dis

2020, Vol. 14: 1–17

DOI: 10.1177/1753466620971143

Abstract

Background: There are two US Food and Drug Administration (FDA)-approved drugs, pirfenidone and nintedanib, for treatment of patients with idiopathic pulmonary fibrosis (IPF). However, neither of these drugs provide a cure. In addition, both are associated with several drug-related adverse events. Hence, the pursuit for newer IPF therapeutics continues. Recent studies show that joint analysis of systems-biology-level information with drug–disease connectivity are effective in discovery of biologically relevant candidate therapeutics.

Methods: Publicly available gene expression signatures from patients with IPF were used to query a large-scale perturbagen signature library to discover compounds that can potentially reverse dysregulated gene expression in IPF. Two methods were used to calculate IPF–compound connectivity: gene expression-based connectivity and feature-based connectivity. Identified compounds were further prioritized if their shared mechanism(s) of action were IPF-related.

Results: We found 77 compounds as potential candidate therapeutics for IPF. Of these, 39 compounds are either FDA-approved for other diseases or are currently in phase II/III clinical trials suggesting their repurposing potential for IPF. Among these compounds are multiple receptor kinase inhibitors (e.g. nintedanib, currently approved for IPF, and sunitinib), aurora kinase inhibitor (barasertib), epidermal growth factor receptor inhibitors (erlotinib, gefitinib), calcium channel blocker (verapamil), phosphodiesterase inhibitors (roflumilast, sildenafil), PPAR agonists (pioglitazone), histone deacetylase inhibitors (entinostat), and opioid receptor antagonists (nalbuphine). As a proof of concept, we performed *in vitro* validations with verapamil using lung fibroblasts from IPF and show its potential benefits in pulmonary fibrosis.

Conclusions: As about half of the candidates discovered in this study are either FDA-approved or are currently in clinical trials for other diseases, rapid translation of these compounds as potential IPF therapeutics is possible. Further, the integrative connectivity analysis framework in this study can be adapted in early phase drug discovery for other common and rare diseases with transcriptomic profiles.

The reviews of this paper are available via the supplemental material section.

Keywords: idiopathic pulmonary fibrosis, IPF, pulmonary fibrosis, drug discovery, drug repositioning, verapamil, computational drug discovery

Received: 8 July 2020; revised manuscript accepted: 5 October 2020.

Correspondence to:
Anil G. Jegga
Cincinnati Children's Hospital Medical Center, 240 Albert Sabin Way, MLC 7024, Cincinnati, OH 45229, USA

Department of Computer Science, University of Cincinnati College of Engineering, Cincinnati, OH, USA

Department of Pediatrics, University of Cincinnati College of Medicine, Cincinnati, OH, USA
anil.jegga@cchmc.org

Yunguan Wang
Division of Biomedical Informatics, Cincinnati Children's Hospital Medical Center, Cincinnati, OH, USA

Jaswanth K. Yella
Sudhir Ghandikota
Division of Biomedical Informatics, Cincinnati Children's Hospital Medical Center, Cincinnati, OH, USA

Department of Computer Science, University of Cincinnati College of Engineering, Cincinnati, OH, USA

Tejaswini C. Cherukuri
Division of Pulmonary Medicine, Cincinnati Children's Hospital Medical Center, Cincinnati, OH, USA

Harshavardhana H. Ediga
Division of Pulmonary Medicine, Cincinnati Children's Hospital Medical Center, Cincinnati, OH, USA

Department of Biochemistry, National Institute of Nutrition, Hyderabad, Telangana, India

Satish K. Madala
Division of Pulmonary Medicine, Cincinnati Children's Hospital Medical Center, Cincinnati, OH, USA

Department of Pediatrics, University of Cincinnati College of Medicine, Cincinnati, OH, USA

Introduction

Idiopathic pulmonary fibrosis (IPF), a chronic and fatal fibrotic lung disease in people over 50 years old is estimated to affect 14–42.7 per 100,000 people.[1] IPF is characterized by progressive subpleural and paraseptal fibrosis, heterogeneous honeycomb cysts (honeycombing), and clusters of fibroblasts and myofibroblasts.[2] The median survival time of patients with IPF is 2.5–3.5 years, with 5-year survival rate around 20%.[1] Currently, two small molecules (pirfenidone and nintedanib) are approved for IPF and are reported to slow down lung function decline caused by disease progression. However,

drug-induced side-effect profiles of these two drugs are formidable and their therapeutic effects are suppressive rather than pulmonary fibrosis remission or reversal.[3,4] The pursuit for safer and efficacious therapies or combinatorials that arrest, or reverse fibrosis therefore continues. On the other hand, technological advances in experimental and computational biology resulted in rapidly expanding genomic and biomedical data, including transcriptomic profiles of disease and small molecules, disease or drug associated pathways and protein–protein interactions.[5–7] Various approaches have been developed to facilitate *in silico* drug discovery *via* joint analysis of these data including the widely used connectivity mapping approach.[8]

The concept of connectivity mapping between a drug and a disease is defined as the gene expression-based similarity calculated using a Kolmogorov–Smirnov statistic-like algorithm.[9,10] It was first introduced as the ConnectivityMap (CMap)[8] and succeeded by the Library of Integrated Network-Based Cellular Signatures (LINCS) L1000 project (CLUE platform),[8,11] which currently contains gene expression profiles of ~20,000 small molecule perturbagens analyzed in up to 72 cell lines. The connectivity mapping concept and application have led to the discovery of novel candidate compounds for disease, drug repurposing candidates, and novel drug mechanism of actions.[12–16]

Recently, similar *in silico* drug discovery approaches for IPF have been reported, wherein joint analysis of systems-biology-level information with drug–IPF connectivity are used to discover biologically relevant candidate therapeutics for IPF. For instance, Karatzas *et al.* developed a scoring formula to evaluate drug–IPF connectivity obtained from multiple sources and identified several IPF candidate therapeutics.[17] Interestingly, neither of the two approved IPF drugs (pirfenidone and nintedanib) was re-discovered by their approach.[17] In another recent study using network-based approach and integrated KEGG network with connectivity analysis sunitinib, dabrafenib and nilotinib were identified as potential repurposing candidates for IPF.[18]

Using a similar approach, namely, by examining connectivity between IPF gene signature and LINCS small molecules, we have previously reported 17-AAG (a known Hsp90 inhibitor) as a potential candidate therapeutic that inhibits fibroblast activation in a mouse model of pulmonary fibrosis.[14] In another study, we screened connectivity of LINCS small molecules with cystic fibrosis (CF) and integrated with systems-biology-level information from CFTR to identify a candidate therapeutic for CF.[13] These results suggest that disease–drug connectivity complemented with systems-biology-level information of drugs and disease could enable candidate therapeutic discovery. In the current study, we therefore calculated both gene expression and enriched pathway-based connectivity between IPF and small molecules in a semi-supervised manner and integrated these results with cheminformatics knowledge to prioritize candidate therapeutics for IPF. We identified 77 (out of ~20,000 LINCS small molecules) candidate therapeutics for IPF. Significantly, among these 77 compounds was the approved drug for IPF (nintedanib), as well as several other compounds that are either currently being investigated or reported as a potential candidate therapeutics for IPF or investigated in clinical trial and reported to be ineffective (sunitinib, nilotinib, and sildenafil). *In vitro* and *in vivo* preclinical studies have reported beneficial effects of histone deacetylase (HDAC) inhibitors (HDACIs) in preventing or reversing fibrogenesis.[19,20] Likewise, previous studies reported the beneficial effects of calcium channel blocking in bleomycin-induced pulmonary fibrosis.[21,22] All these results suggest that the current approach has the potential to identify "true" candidate therapeutics. In the current study, we have selected verapamil, a US Food and Drug Administration (FDA)-approved calcium channel blocker, from our computational screening results for *in vitro* validation.

Methods

IPF studies/cohort selection

We used publicly available gene expression profiles from the Gene Expression Omnibus (GEO)[23] database for generating IPF gene expression signatures. As gene expression profiles are known to be heterogeneous in different patients,[24,25] we selected six GEO datasets comparing primary healthy human lung tissues with primary IPF lung tissues for this study to potentially mitigate such heterogeneity (Figure 1 and Table 1).

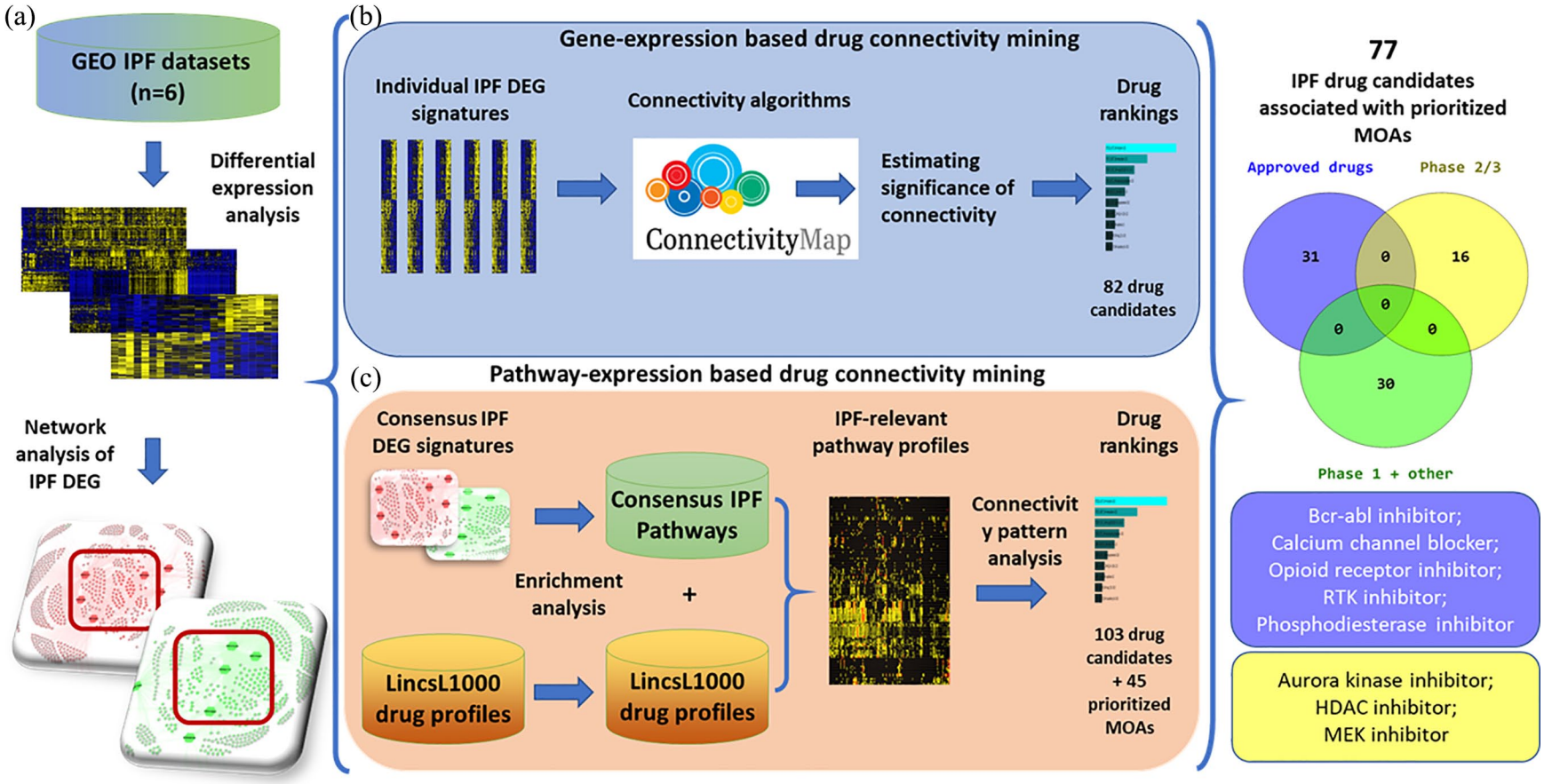

Figure 1. Overview of expression and annotation-based connectivity analysis. Workflow in this study could be summarized into three steps. (a) Collection and differential analysis of human IPF gene expression datasets; (b) Expression-based connectivity analysis through CLUE platform; (c) annotation-based connectivity analysis examining similarity between pathways perturbed by compounds and those involved in IPF.
IPF, idiopathic pulmonary fibrosis.

Table 1. Summary of six datasets comparing IPF lung tissue with healthy controls.

GEO dataset identifier	Sample description	Reference
GSE10667	23 IPF samples and 16 controls	Konishi *et al.*; Rosas *et al.*[26,27]
GSE24206	17 IPF samples and 6 controls	Meltzer *et al.*[28]
GSE48149	13 IPF samples and 9 controls	Hsu *et al.*[29]
GSE53845	40 IPF samples and 8 controls	DePianto *et al.*[24]
GSE47460	131 IPF samples and 12 controls*	LGRC
GSE101286	7 IPF samples and 3 controls	Horimasu *et al.*[30]

*Only 12 control samples in the LGRC dataset with 'normal' clinical and pathological diagnosis were used as control.
GEO, Gene Expression Omnibus; IPF, idiopathic pulmonary fibrosis; LGRC, Lung Genomics Research Consortium.

Differential analysis of IPF gene expression profiles

Differential analysis was performed in R in using the package LIMMA (linear models for microarray data).[31] Genes with fold change $\geqslant 1.5$ and adjusted p-value $\leqslant 0.05$ were considered differentially expressed. Each dataset was analyzed separately.

Known pulmonary fibrosis genes. We compiled 3278 "known" pulmonary fibrosis genes from literature and several data resources (Supplemental Table 1). This list contains human genes associated with "Pulmonary fibrosis", "Idiopathic pulmonary fibrosis" and "Interstitial Lung Disease" from Open Targets platform,[32] CTD,[33] Phenopedia,[34] and GeneCards[35] databases.

IPF–compound connectivity estimation and permutation analysis

To correct for multiple testing problem introduced by conducting connectivity analysis (Figure 1) in multiple datasets, we used permutation analysis to estimate the significance of connectivity. First, we constructed a matrix of connectivity score, denoted by s, between CLUE compound $\boldsymbol{i}$ and IPF dataset $\boldsymbol{d}$ in cell line $\boldsymbol{j}$. Next, positive, and negative connectivity to IPF were determined by thresholding connectivity score at 90 and −90, respectively:

$$c_{i,d,j} = \begin{cases} 1, \left(s_{i,d,j} \geq 90\right) \\ 0, \left(-90 < s_{i,d,j} < 90\right) \\ -1, \left(s_{i,d,j} \leq -90\right) \end{cases}$$

Overall connectivity, denoted by o, between each compound to IPF across all cell lines is summarized as the sum of individual connectivity across all datasets and all cell lines:

$$o_i = \sum_{d}^{m} \sum_{j}^{n} c_{i,d,j}$$

Permutation was performed by randomly shuffling rows of the connectivity matrix **C**, so that compound names were randomly assigned. Then, the permutated overall compound-to-IPF connectivity **O'** scores were calculated, and we recorded incidences where $o_i \leq o_i'$, which indicates the observed compound to IPF connectivity is not larger than random connectivity:

$$f_{ip} = \begin{cases} 1, \left(o_i \leq o_i'\right) \\ 0, \left(otherwise\right) \end{cases}$$

We repeated the permutation tests for 100,000 times and estimated significance as the frequency of **F** over all permutations. The significance cut-off was set at 0.05.

Functional enrichment

Functional enrichment analysis was performed using pre-compiled gene annotation libraries from the ToppGene Suite.[36] Enrichment p-values were calculated using hypergeometric test in Python using the SciPy package.

Annotation-based connectivity analysis

Annotation-based compound–IPF connectivity (Figure 1) was generated and evaluated as follows:

(1) Identify enriched annotation terms in conserved IPF genes (genes that were differentially expressed in more than four IPF datasets) resulting in two vectors, $\boldsymbol{I_{up}}$ and $\boldsymbol{I_{down}}$;
(2) Calculate enrichment score, $\boldsymbol{P_{i,up}}$ and $\boldsymbol{P_{i,down}}$, using the 500 top and 500 bottom genes of each LINCS L1000 small molecule expression profile, denoted by **i**, in the upregulated and downregulated IPF pathways identified in step (1);
(3) Calculate annotation-based connectivity score, defined as Pearson correlation between $\boldsymbol{P_{i,up}}$ and $\boldsymbol{I_{down}}$, and between $\boldsymbol{P_{i,down}}$ and $\boldsymbol{I_{up}}$;
(4) To correct for false positives from multiple testing, permutation analysis were performed by swapping annotation terms in $\boldsymbol{P_{i,down}}$ and $\boldsymbol{P_{i,up}}$, followed up recalculation of annotation-based connectivity. 100,000 permutations were performed with significance threshold set to 0.05.

Primary lung fibroblast cultures and RT–PCR. IPF lungs were collected in Dulbecco's modified eagle medium (DMEM) containing 10% FBS (Life Technologies, NY, USA) from the Interstitial Lung Disease Biorepository at the University of Michigan Medical School following the IRB regulations of the institute. Lung pieces were finely minced with sterile razor blades and incubated at 37°C for 30 min in 5 ml of DMEM containing collagenase (2 mg/ml). Digested tissue was passed through a 100-μm filter, washed twice with DMEM medium, plated onto 100 mm tissue-culture plates, and incubated at 37°C, 5% CO_2 to allow cells to adhere and migrate away from larger remaining tissue pieces. Adherent primary lung fibroblasts were collected on day 5 or 8 and lung-resident fibroblasts were isolated with a negative selection using anti-CD45 beads as described earlier (JCI insight 2018). These fibroblasts were used for drug treatment studies up to passage four or less. After drug treatments, total RNA was extracted using RNAeasy Mini kit (QIAGEN Sciences, Valencia, CA, USA) and polymerase chain reaction with reverse transcription (RT–PCR) assays were performed. Relative quantities of messenger RNA for several genes were determined using SYBR Green PCR Master Mix (Applied Biosystems) and target gene transcripts in each sample were normalized to glyceraldehyde 3-phosphate dehydrogenase (GAPDH) and expressed as a relative increase or decrease compared with controls. As expected, we observed no changes in the copy number of GAPDH in IPF fibroblasts treated with verapamil compared with vehicle [0.0001 % dimethyl sulphoxide (DMSO)]. Also, we performed melt curve analysis to exclude primer sets producing nonspecific PCR products. RT–PCR primer sequences for genes, GAPDH (fwd: AGCCACATCGCTCAGACAC; rev: GCCCAATACGACCAAATCC), Col1α1 (fwd: GGGATT CCCTGGACCTAAAG; rev: GGAACACCTCGCTCTCCA), Col3α1 (fwd: CTGGACCCCA GGGTCTTC; rev: CATCTGATCCAGGGTTT CCA), Col5α1 (fwd: CAGCCCGGAGAGAACAGA; rev: GGTGCAGCTAGGTCATGTGAT), αSMA (fwd: GCTTTCAGCTTCCCTGAACA; rev: GGAGCTGCTTCACAGGATTC) and FN1 (fwd: CTGGCCGAAAATACATTGTAAA; rev: CCACAGTCGGGTCAGGAG).

Results

Differential expression analysis of IPF datasets

We analyzed six gene expression datasets comparing gene expression of IPF lung tissue with healthy controls (Table 1). Differential expression analysis was performed in each dataset using the R package LIMMA. Differentially expressed genes (DEGs) were defined as genes with fold change $\geqslant$1.5 and Benjamini–Hochberg false discovery rate adjusted p-value $\leqslant$0.05. The number of DEGs ranged from 263 to 2385, and 4677 genes were unambiguously upregulated, and 2210 genes were unambiguously downregulated in at least one IPF dataset [Figure 2(a); Supplemental Table 1]. Overall similarity between DEG gene lists was low, as reflected by the median Jaccard index between gene lists (0.077). While the lack of concordance between datasets suggests disease heterogeneity in IPF, it also provides the rationale for meta-analysis using multiple datasets to extract high confidence drug candidates for IPF. Despite the overall heterogeneity in DEGs among different IPF datasets, there were also a considerable number of genes that were consistently dysregulated in four or more IPF datasets. We call these "conserved" IPF genes (197 upregulated genes and 84 downregulated genes). Among these conserved DEGs, 179 genes (121 upregulated and 58 downregulated) were known previously to be involved in pulmonary fibrosis [Figure 2(b)]. Functional enrichment analysis of conserved IPF

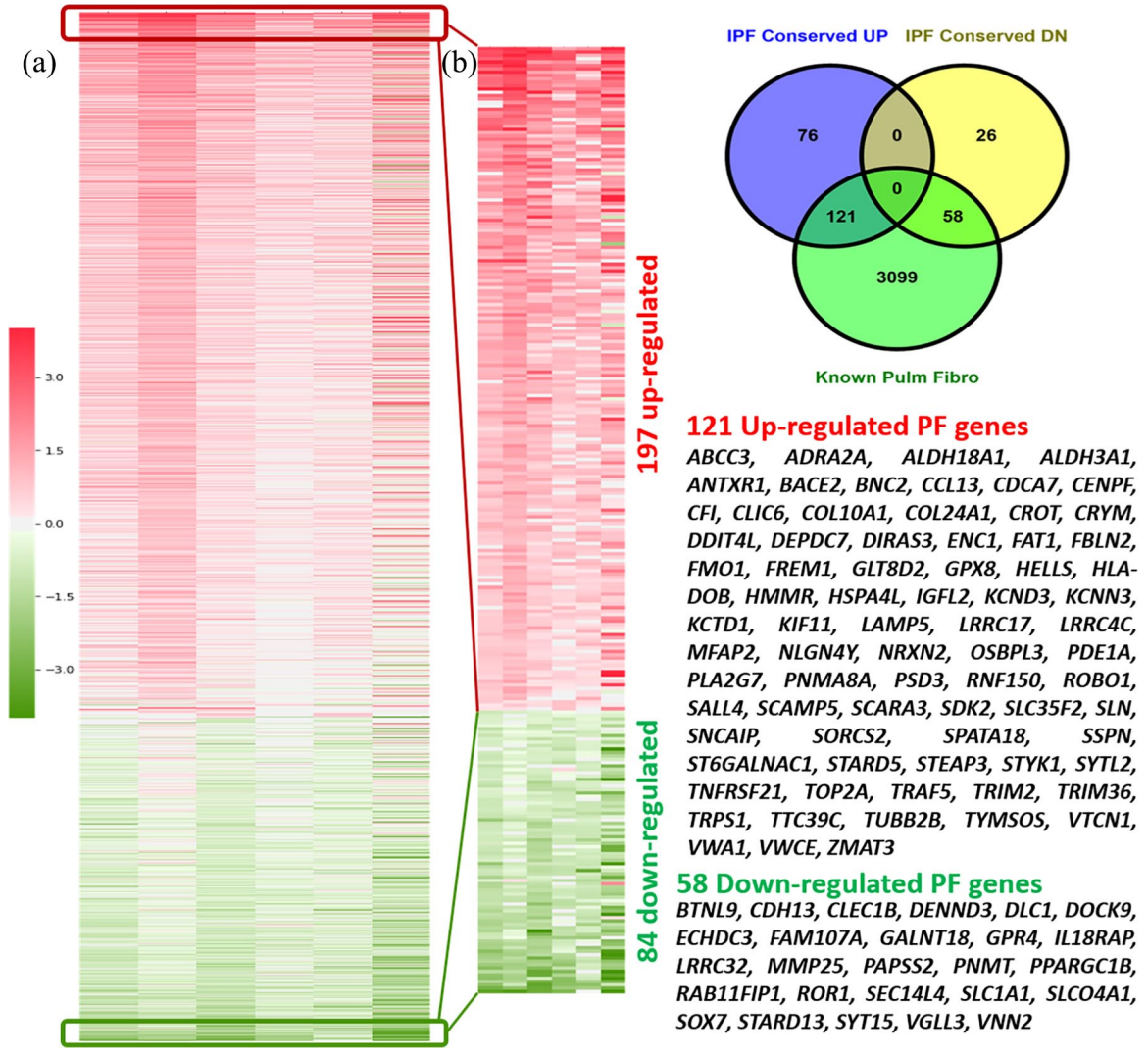

Figure 2. Heat map view of differentially expressed genes in six IPF datasets. (a) Expression of 2206 genes unambiguously differentially expressed in at least two IPF dataset are shown. Genes are represented in rows and patient samples in columns. Cells in heat map were sorted discerningly based on median log fold change in six datasets and on number of datasets they were differentially expressed in. (b) Genes that were upregulated or downregulated in at least four datasets. Intersection with all known pulmonary fibrosis genes are shown in the Venn diagram.
IPF, idiopathic pulmonary fibrosis.

genes showed that biological processes involved in extracellular matrix formation, inflammation responses and cell migration were upregulated, whereas processes involved in normal lung processes such as angiogenesis and alveolar functions were downregulated.

Expression-based connectivity analysis and permutation analysis

We used the National Institutes of Health LINCS as the compound search space for IPF candidate therapeutics. The LINCs Touchstone dataset has a total of approximately 8400 perturbagens, including more than 2000 small molecules that have produced gene signatures generated from testing on a panel of nine cell lines. These cell lines include A375, A549, HEPG2, HCC515, HA1E, HT29, MCF7, PC3, and VCAP. LINCS has expression profiles of ~20,000 small molecules assayed in various cell lines. To find potential IPF candidate therapeutics, we adopted the connectivity mapping method, which assumes small molecules with gene expression profiles negatively correlated with that

Table 2. List of 39 potential repurposing candidates for IPF.

Compound	IPF-related mechanism of action	Indication	Phase
febuxostat	xanthine oxidase inhibitor	hyperuricemia	Approved
nortriptyline	tricyclic antidepressant	depression	Approved
amsacrine	topoisomerase inhibitor	cancer	Approved
irinotecan	topoisomerase inhibitor	cancer	Approved
camptothecin	topoisomerase inhibitor	cancer	phase III
pioglitazone	PPAR receptor agonist, insulin sensitizer	diabetes mellitus	Approved
roflumilast	phosphodiesterase inhibitor	COPD	Approved
sildenafil	phosphodiesterase inhibitor	Erectile dysfunction and pulmonary hypertension	Approved
nalbuphine	opioid receptor antagonist	pain relief	Approved
everolimus	mTOR inhibitor	cancer	Approved
sunitinib	mRTK inhibitor	cancer	Approved
nintedanib	mRTK inhibitor	IPF	Approved
dovitinib	mRTK inhibitor	cancer	phase III
pazopanib	mRTK inhibitor	cancer	Approved
selegiline	monoamine oxidase inhibitor	Parkinson's disease	Approved
selumetinib	MEK inhibitor	cancer	phase III
curcumin	lipoxygenase inhibitor, histone acetyltransferase inhibitor, cyclooxygenase inhibitor		Approved
tomelukast	leukotriene receptor antagonist	asthma	phase III
dasatinib	mRTK inhibitor	cancer	Approved
lafutidine	histamine receptor antagonist	duodenal ulcer disease, peptic ulcer disease	Approved
ranitidine	histamine receptor antagonist	heartburn	Approved
amodiaquine	histamine receptor agonist	malaria	Approved
entinostat	HDAC inhibitor	cancer	phase III
remacemide	glutamate receptor antagonist	epilepsy and neurodegenerative diseases	phase III
riluzole	glutamate inhibitor	amyotrophic lateral sclerosis	Approved
erlotinib	EGFR inhibitor	cancer	Approved
gefitinib	EGFR inhibitor	cancer	Approved
sulpiride	dopamine receptor antagonist	schizophrenia	Approved

(Continued)

Table 2. (Continued)

Compound	IPF-related mechanism of action	Indication	Phase
mycophenolic acid	dehydrogenase inhibitor, inositol monophosphatase inhibitor	organ rejection	Approved
ketorolac	cyclooxygenase inhibitor	NSAID	Approved
mestinon	cholinesterase inhibitor	myasthenia gravis	Approved
fipronil	chloride channel blocker	insecticide	Approved
verapamil	calcium channel blocker	hypertension	Approved
gaboxadol	benzodiazepine receptor agonist	insomnia	phase III
ivermectin	benzodiazepine receptor agonist	gastrointestinal parasites	Approved
nilotinib	Bcr-Abl kinase inhibitor	cancer	Approved
barasertib-HQPA	aurora kinase inhibitor	cancer	phase II/ phase III
regadenoson	adenosine receptor agonist	myocardial perfusion imaging	Approved
bucladesine	adenosine receptor agonist	skin ulcer	Approved

COPD, chronic obstructive airways disease; EGFR, epidermal growth factor receptor; HDAC, histone deacetylase; IPF, idiopathic pulmonary fibrosis; NSAID, nonsteroidal anti-inflammatory drug.

of a disease are likely to be therapeutic for the disease. We first queried the Connectivity Map web platform (CLUE.io) for compounds with a reversed gene expression profile compared to IPF. From each dataset, a gene signature having up to 150 most upregulated and downregulated genes was extracted and used to query the CLUE platform (Supplemental Table 2). Using the hits from CLUE results, we applied a "greedy" approach to capture the highest number of compounds connected to IPF by selecting compounds with at least 90 connectivity score in any one of the cell lines. This approach returned 1000+ compounds that relate to IPF at least once. However, this approach results in several compounds that are connected to IPF in both directions, that is, potentially inducing, and reversing IPF gene expression profiles at the same time [Figure 3(a)]. This suggests that the gene expression perturbation due to technical variation is present in our data and is reflected in the form of these low-frequency compounds in CLUE analysis. Based on the assumption that IPF-related gene expression patterns are consistently present in our selected six IPF datasets, we performed permutation analysis to estimate the significance of IPF disease connectivity and filter out potential false positives. With a 0.05 significance cut-off, we found 82 compounds that were significantly connected with IPF [Figure 3(b)]. These compounds were associated with 63 different known drug mechanisms of action.

Functional enrichment-based connectivity analysis

A major limitation of using the Touchstone Library-based CLUE platform to screen for drug candidates is that it only covers 2836 out of ~20,000 small molecules available in the full L1000 database. To overcome this, we searched for IPF candidate therapeutics among the remaining ~17,000 LINCS small molecules. To do this, we used a functional enrichment-based metric to evaluate drug–IPF connectivity of these LINCS small molecules, wherein gene expression data from both the compound and the IPF datasets were transformed into enrichment p-values using hypergeometric tests against gene functional annotations (Gene Ontology Biological Process, Mouse Phenotypes and KEGG pathways). To minimize the noise introduced by biological processes not relevant to IPF, we only considered functional annotations enriched in the conserved IPF gene sets, and thus, each compound

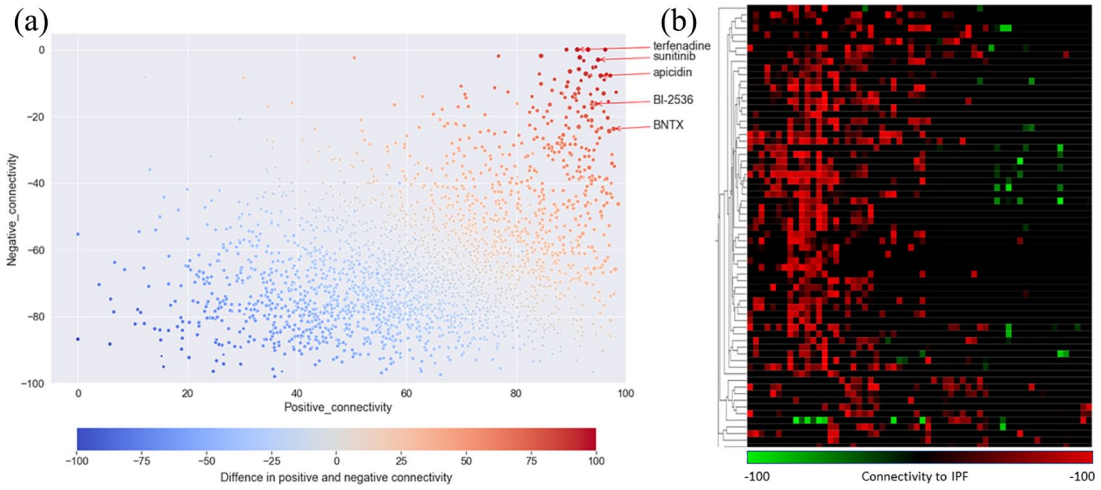

Figure 3. Gene expression-based connectivity score of CLUE compounds. (a) Scatter-plot of positive connectivity score against negative connectivity score between each CLUE compound and each IPF dataset across all cell lines. Coordinates of each point were determined by the average of highest or lowest six connectivity scores among all 54 values across six IPF datasets and nine cell lines in CLUE. (b) Heat map view of connectivity score of 82 compounds that were significantly connected to IPF based on permutation analysis. IPF, idiopathic pulmonary fibrosis.

enrichment profile was limited to these pathways. Connectivity between a compound and IPF was defined as the cosine similarity between the *p*-values of pathways enriched in compound u-regulated genes and those enriched in IPF downregulated genes, and vice versa. Next, we used permutation analysis as discussed in the earlier sections to estimate the significance of the feature-based compound–IPF connectivity and identified 345 compounds that perturbed IPF-related pathways in an overall opposite manner compared with IPF. To find groups of functionally related therapeutic candidates that could act on IPF-perturbed biological processes, we performed clustering analysis on the compound enrichment profiles and prioritized four clusters of compounds with high connectivity to IPF. The compounds in three clusters selectively downregulated pathways such as 'cell adhesion', 'collagen metabolic process' and 'regulation of programmed cell death', which were all upregulated in IPF. On the other hand, compounds in the cluster that showed upregulation of 'blood vessel morphogenesis' and 'angiogenesis' were downregulated in IPF. The approved IPF drug, nintedanib was in this cluster of compounds. Combining compounds from these four clusters, we found 103 candidates as IPF therapeutic candidates from annotation- or feature-based connectivity analysis (Figure 4). These compounds include epidermal growth factor receptor (EGFR) inhibitor gefitinib, platelet-derived growth factor receptor (PDGFR) and vascular endothelial growth factor receptor (VEGFR) inhibitor dovitinib, and KIT inhibitor sunitinib.

Prioritization of IPF candidate therapeutics based on shared mechanism of action

In the annotation-based connectivity analysis, we observed that most of the discovered compounds shared drug mechanisms of action (MOA). For instance, EGFR inhibition, PDGFR inhibition and VEGFR inhibition were shared across multiple compounds suggesting potential relevance of these MOAs to IPF. This also suggests a likelihood of higher therapeutic potential of multiple compounds with shared or similar MOAs. Leveraging the known MOA information of the discovered compounds, we further prioritized compounds belonging to MOA that were prioritized by annotation-based connectivity analysis. After excluding glucocorticoid receptor agonists and immunosuppressants from the list because of their known detrimental effects in IPF, we found 48 MOAs meeting these criteria (Supplemental Table 3). Based on these MOAs, we selected 77 compounds as our final preclinical candidates for IPF (Supplemental Table 4). Among these, 39 were FDA-approved drugs or

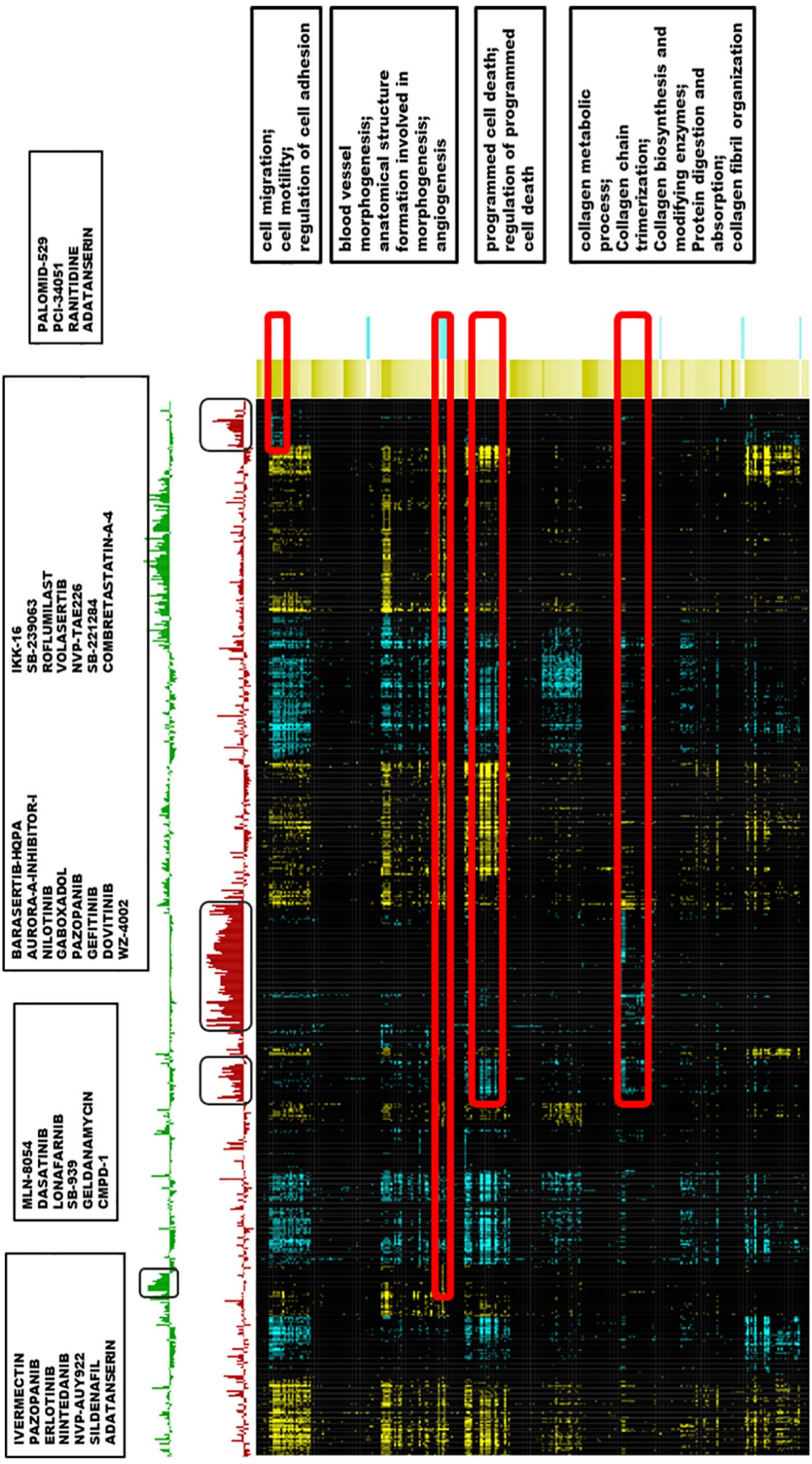

Figure 4. Enriched pathway heat map view of 345 drugs significantly connected to IPF in annotation-based connectivity analysis. Enrichment terms in categories including KEGG pathways, Wiki pathways, REACTOME, Mouse phenotype and Gene Ontology: Biological process in either consistently upregulated or downregulated IPF genes are arranged in rows. LINCS drug profiles were arranged in columns. Blue indicates annotation terms are enriched in downregulated genes by drug or IPF, and yellow indicates annotation terms are enriched in upregulated genes by drug or IPF. K-means clustering was used to identify compound modules.
IPF, idiopathic pulmonary fibrosis; LINCS, Library of Integrated Network-Based Cellular Signatures.

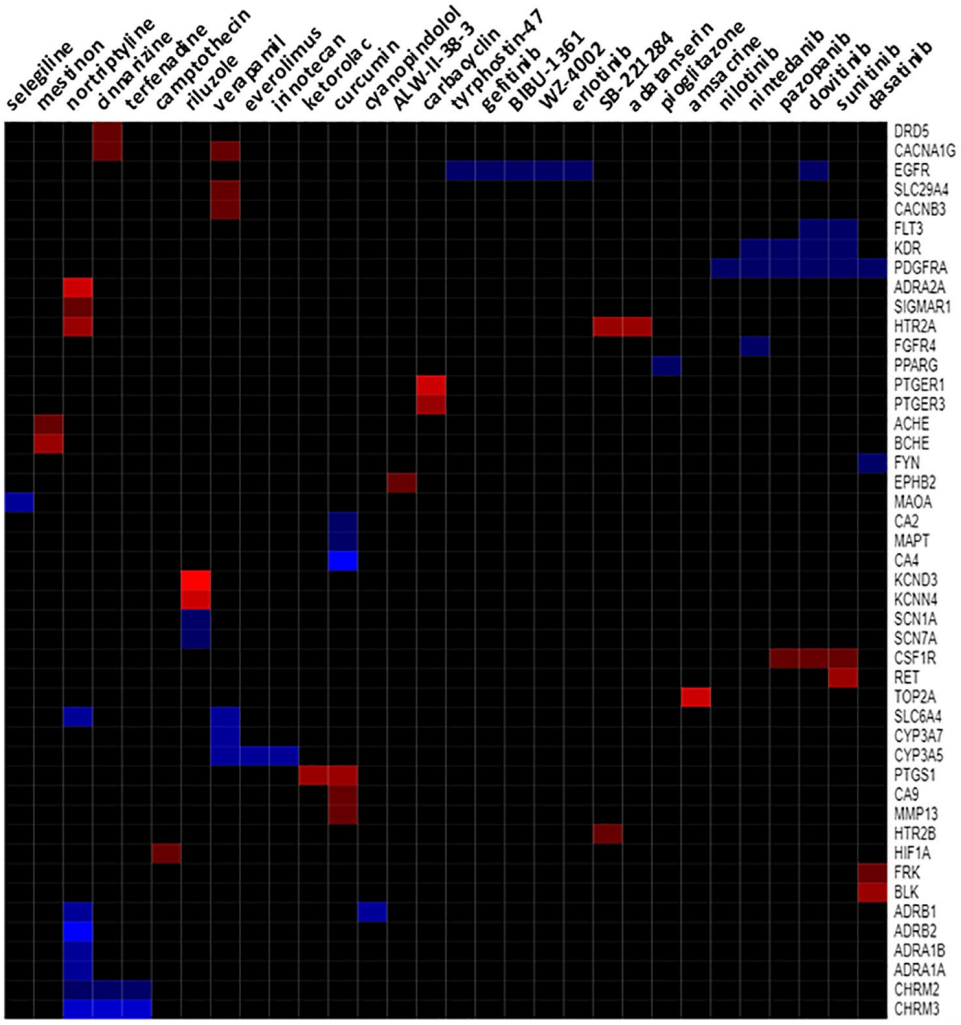

Figure 5. Heat map view of candidate compound targets that are differentially expressed in IPF. Log fold changes of 48 target genes of 30 compounds in IPF are shown. Only compounds with targets differentially expressed in at least two IPF datasets are included. Differentially expressed drug targets in IPF are in rows and discovered IPF candidate compounds are in columns. Rows and columns are ordered using two-dimensional hierarchical clustering.
IPF, idiopathic pulmonary fibrosis.

phase II/III compounds suggesting their repositioning potential for IPF (Table 2). These drugs include Bcr-Abl kinase inhibitors, EGFR inhibitors, opioid receptor inhibitors, receptor tyrosine kinase (RTK) inhibitors and aurora kinase inhibitors. Notably, the approved IPF drug nintedanib was also among this list. This is important because nintedanib was not included in the CLUE database and would have been missed if annotation-based connectivity was not examined. A closer look at the pharmacological targets of these candidates revealed that many of these targets such as PDGFRA, EGFR, FGFR4, FYN and KDR were differentially expressed in IPF. Similarly, CACNA1G, SLC29A4, CACNB3, SLC6A4 (all targets of verapamil, a known calcium channel blocker), were differentially expressed in IPF. Among these targets, KDR, FGFR4 and PDGFRA are associated with nintedanib and other multi-targeted RTK inhibitors such as dovitinib, pazopanib and sunitinib (Figure 5). These genes are involved in VEGF and PI3K/AKT signaling and VEGFR2 mediated cell proliferation, suggesting a role for multi-targeted RTK inhibitors in controlling IPF through VEGF signaling inhibition.

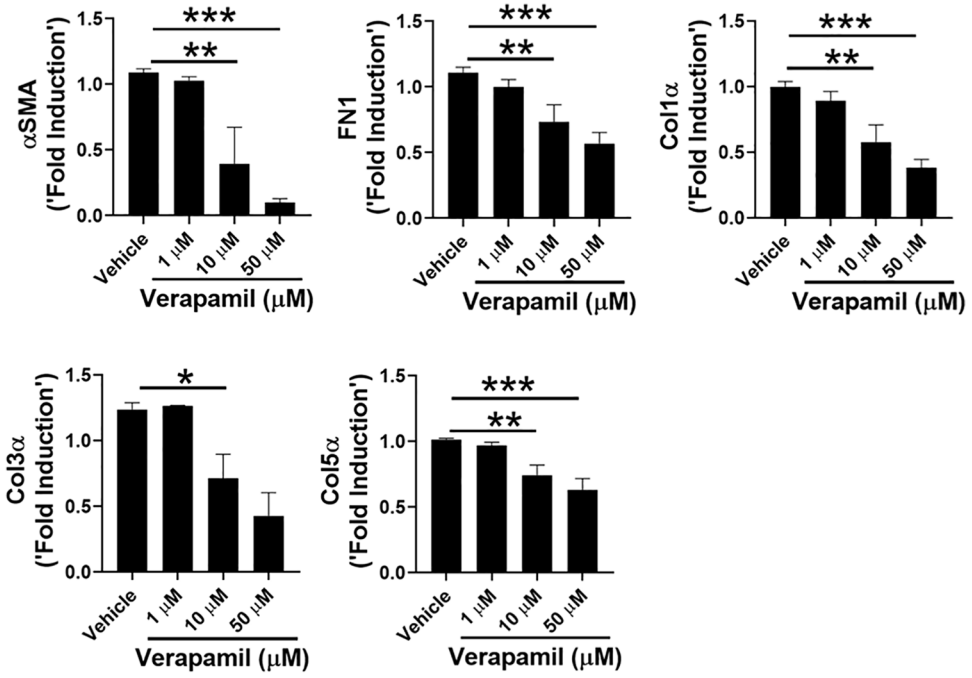

Figure 6. Verapamil treatment attenuates pro-fibrotic gene expression. IPF fibroblasts were treated with either vehicle (DMSO 0.001%) or verapamil (1, 10 and 50 μM) for 16 h. Total RNA was analyzed for the expression of αSMA and ECM genes (FN1, Col1α, Col3α and Col5α) using RT–PCR. *$p < 0.05$; **$p < 0.005$ ***$p < 0.0005$; ****$p < 0.00005$.

DMSO, dimethyl sulphoxide; IPF, idiopathic pulmonary fibrosis; RT–PCR, polymerase chain reaction with reverse transcription.

Antifibrotic potential of verapamil. Calcium channel blockers are commonly used in clinical practice and reported to be well tolerated. Therefore, in the current study, as a proof of concept, we have selected verapamil, a known calcium channel blocker and anti-hypertension drug, from our computational screening results for *in vitro* validation. IPF lung fibroblasts were treated with either vehicle (0.001% DMSO) or verapamil (Figure 6). We observed a significant reduction in the expression of fibroproliferative genes including fibronectin 1 (*FN1*), collagens (*COL1A1*, *COL3A1*, and *COL5A1*), and αSMA with verapamil treatment for 16 h. compared to vehicle treated IPF fibroblasts (Figure 6). The doses of verapamil used did not affect viability of IPF fibroblasts suggesting antifibrotic effects of verapamil observed above may not be due to cell death or drug toxicity (Supplemental Figure 1). These findings support the premise that candidate small molecules found using *in silico* screening methods are potentially effective in inhibiting fibroblast activation and may serve as potential drug candidates for further validation using *in vitro* and *in vivo* preclinical IPF models. Testing of additional candidates, however, is warranted.

Discussion

In this study, we developed a multiplexed, generalizable approach to discover novel therapeutics by integrating disease-driven and perturbagen-driven gene expression profiles, disease-associated biological pathways, and cheminformatics of perturbagen. Compound–IPF connectivity was examined from different dimensions including transcriptome, functional enrichment profiles, and drug mechanisms of actions. With this approach, we not only identified approved IPF therapeutic drugs (nintedanib) but also identified additional FDA-approved drugs that share similar MOA as IPF candidate therapeutics. Notably, these drugs were not discoverable using conventional transcriptome-based connectivity analysis alone. Further, approved drugs or investigational compounds associated with MOAs such as Bcr-Abl inhibitor and aurora kinase inhibitor, were also among our

candidate list, which could provide insights into novel intervention strategies against IPF.

Transcriptome-based connectivity mapping was first introduced more than a decade ago and has been applied to facilitate drug discovery for various diseases, including IPF. In a recent study, Karatzas *et al.* proposed nine drugs as IPF therapeutics based on their connectivity with expression profiles derived from IPF datasets. However, they were not able to re-discover approved IPF drugs although these drugs were included in the LINCS L1000 that was queried.[17] Likewise, our gene expression-based connectivity approach through CLUE prioritized 82 small molecules as IPF therapeutics candidates, but neither of the FDA-approved IPF drugs (pirfenidone or nintedanib) was in the list. A closer look at the connectivity scores revealed that pirfenidone, one of the two approved IPF therapeutics, had no connectivity to IPF in any of the six queried datasets. There could be several reasons for this. Our method uses transcriptomic profiles of IPF to find candidate drugs. It is possible that drugs that have minimal effect on IPF-specific gene signature or alter translational modifications involved in fibrotic processes may not be captured as top candidates in this approach. The mechanisms underlying pirfenidone action have remained largely unknown.[37] Another possible reason could be the heterogeneity in the gene signature based on whole lung tissue from IPF. As part of ongoing and future work, we plan to undertake the computational screening using transcriptomic data from the single-cell RNA-sequencing studies.[38–40] Interestingly, pirfenidone was connected to verapamil (transcriptionally similar, based on gene expression profiles of compounds in Clue.io platform). Our preclinical *in vitro* validations with verapamil using human IPF lung fibroblast revealed therapeutic benefit of verapamil in IPF. Earlier studies reported the beneficial effects of calcium channel blocking in bleomycin-induced pulmonary fibrosis.[21,22] However, more studies are warranted to test therapeutic efficacy of verapamil singly or in combination with pirfenidone using experimental models of fibrotic lung disease. In addition, mining electronic health records and side-effects data (FDA's adverse events reporting system) for testing whether patients under both therapy have a better response are part of our related ongoing studies.[41] Nintedanib, the second approved therapeutic for IPF, was not included in CLUE and therefore we were unable to assess its connectivity to IPF using the Clue.io platform.

We also examined the connectivity between IPF and the ~17,000 compounds not covered in the Clue.io platform. The gene expression profiles associated with these ~17,000 small molecules are from distinct selections of cell lines. Therefore, direct connectivity mapping analysis may be susceptible to biological variation introduced by different cell lines. In addition, it has been shown that integration of prior knowledge, particularly in the form of gene set information in biological pathways, improves the accuracy of drug activity predictions.[42] We evaluated drug–IPF connectivity through enriched pathways directly related to IPF under the assumption that pathways perturbed by drugs are more stable across different host cell conditions compared to individual genes. Annotation-based connectivity analysis lead to discovery of 14 more small molecules that were not included in the CLUE platform. These include aurora kinase inhibitor barasertib-HQPA and phosphodiesterase inhibitor roflumilast. In a recent preclinical study,[43] using two mouse models of pulmonary fibrosis, we have shown barasertib as a possible intervention therapy for IPF. Notably, nintedanib was also among the 14 additional small molecules, and the enriched pathways that contributed to the connection to IPF were related to fibroblast proliferation, ECM production and cell migration, which is in consistent with implicated MOA of nintedanib against IPF *in vitro*.[44]

Among the 77 prioritized candidates, 31 are FDA-approved drugs and are associated with different MOAs. These MOAs include RTK inhibition, which is the known MOA for the approved IPF drug nintedanib. Other compounds with this MOA in our discovered candidate compounds include pazopanib and sunitinib. Sunitinib is approved for treatment of renal cell carcinoma and gastrointestinal stromal tumor, and it has also been shown to be efficacious in inhibiting established pulmonary fibrosis in the bleomycin-induced mouse model.[45] In addition, MOAs involved with these 31 drugs also included those associated with compounds that are currently investigated or are in clinical trial for IPF drugs, such as src-kinase inhibitor and mTOR inhibitor.[46] The MOAs associated with the remaining IPF repositioning candidates included aurora kinase inhibitor, EGFR inhibitor, calcium channel blocker, phosphodiesterase inhibitor, PPAR agonist, Bcr-Abl kinase inhibitors and opioid receptor antagonist. The EGFR pathway plays an important role in pulmonary physiology and chronic

lung diseases[47] and a recent study reported that nintedanib blocks the EGFR paracrine upregulation in IPF.[48] PPAR-α agonists have been shown to attenuate fibrosis in the bleomycin mouse model of pulmonary fibrosis.[49] HDACIs have been reported to improve resolution of pulmonary fibrosis in mice.[19,20] Several studies have shown that calcium channel blockers are useful in animal models of fibrosis in the kidney, heart, liver, and skin (reviewed elsewhere[50]). An earlier study showed that felodipine, a known calcium channel blocker, improved bleomycin-induced decreases in FVC (Forced Vital Capacity) in mice.[22] Verapamil was also shown to reduce scar tissue formation and promote axon growth after peripheral nerve repair.[51] Calcium channel blockers are commonly used in clinical practice, reported to be well tolerated, and are relatively inexpensive. We have recently shown that inhibition of AURKB expression or activity can attenuate fibroblast activation and barasertib, a known AURKB inhibitor attenuates fibrosis in two mouse models of pulmonary fibrosis.[43]

While the computational drug discovery approaches, including the current one, are powerful approaches for preclinical therapeutic discovery and MOA-based hypotheses, they albeit suffer with certain inherent limitations. For example, sildenafil, 1 of the 77 compounds that we have discovered as candidate therapeutics for IPF, has already been investigated in combination with nintedanib in clinical trials[52,53] and was reported to have no significant benefit when compared to patients on nintedanib alone. Nevertheless, discovering a compound (sildenafil) that is tested in a clinical trial for IPF demonstrates the preclinical discovery power of our approach for candidate therapeutics. Second, the current approach is monotherapy-centric and does not consider potential drug–drug interactions. For example, the current approach cannot deduce which of the 77 compounds can be a potential combination compound with nintedanib or pirfenidone. Advanced knowledge mining (e.g. known drug–drug interactions) and machine-learning-based approaches can be potentially explored to address this problem. Third, ours, and other computational approaches do not consider the potential off-target effects leading to adverse events. For example, as a previous study also reported,[21] off-target effects of calcium channel blockers on other cell types cannot be ruled out especially because the lung is composed of more than 50 different cell types with several of these expressing voltage-dependent calcium channels. Three recent single-cell RNA-sequencing studies[38–40] provide high-resolution insights into the cellular architecture of the normal and fibrotic lung. Leveraging the unique cell types from the normal disease lung has the potential to provide novel therapeutic targets for IPF and also prioritize the results from the computational compound screens. Finally, the signatures in LINCS are based on mostly epithelial cell lines, and the compound concentrations used may not be translatable. Hence, further studies are warranted using both *in vitro* and *in vivo* preclinical models of pulmonary fibrosis.

In conclusion, we have developed an integrative connectivity analysis combining information from transcriptomic profiles, disease systems biology and drug cheminformatics for *in silico* IPF drug discovery. Application of our approach earlier in the IPF drug discovery pipeline may help to avert late-stage clinical trial failures. As about half of the candidates we have discovered in this study are FDA-approved or are currently in clinical trials for several diseases, rapid translation of these compounds is possible. Finally, we have suggested novel drug mechanisms that could shed new insights in the search for better IPF drugs.

Author contributions

Y.W. and A.J. conceived this study. Y.W., J.Y. and S.G. collected and analyzed data. Y.W. and A.J. interpreted results from data. T.C., H.E., and S.M. conducted experimental validations. Y.W., S.M. and A.J. edited this manuscript. Y.W. wrote the first draft. All authors took part in the manuscript review and editing.

Availability of data and materials

All data generated or analyzed during this study are included in this published article and its supplementary information files. All supplementary files are also available on the Figshare repository platform (DOI: 10.6084/m9.figshare.12585644; https://figshare.com/articles/IPF_Pan-transcriptome/12585644).

Conflict of interest statement

The authors declare that there is no conflict of interest.

Consent for publication

Not applicable.

Ethics approval and consent to participate

Not applicable.

Funding

The authors disclosed receipt of the following financial support for the research, authorship, and/or publication of this article: This study was supported in part by the National Institutes of Health grants NHLBI 1R21HL133539 and 1R21HL135368 and NCATS 1UG3TR002612 (to AGJ), 1R01 HL134801 (to SKM), US DepartmentofDefensegrantW81XWH-17-1-0666 (to SKM) and by the Cincinnati Children's Hospital and Medical Center.

ORCID iD

Anil G. Jegga https://orcid.org/0000-0002-4881-7752

Supplemental material

The reviews of this paper are available via the supplemental material section.

References

1. Kekevian A, Gershwin ME and Chang C. Diagnosis and classification of idiopathic pulmonary fibrosis. *Autoimmun Rev* 2014; 13: 508–512.
2. Raghu G, Collard HR, Egan JJ, *et al.*; on behalf of the ATS/ERS/JRS/ALAT Committee on Idiopathic Pulmonary Fibrosis. An official ATS/ERS/JRS/ALAT statement: idiopathic pulmonary fibrosis: evidence-based guidelines for diagnosis and management. *Am J Respir Crit Care Med* 2011; 183: 788–824.
3. Richeldi L, du Bois RM, Raghu G, *et al*; INPULSIS Trial Investigators. Efficacy and safety of nintedanib in idiopathic pulmonary fibrosis. *N Engl J Med* 2014; 370: 2071-2082.
4. King TE Jr, Bradford WZ, Castro-Bernardini S, *et al.*; ASCEND Study Group. A phase 3 trial of pirfenidone in patients with idiopathic pulmonary fibrosis. *N Engl J Med* 2014; 370: 2083–2092.
5. Margolis R, Derr L, Dunn M, *et al.* The National Institutes of Health's Big Data to Knowledge (BD2K) initiative: capitalizing on biomedical big data. *J Am Med Inform Assoc* 2014; 21: 957–958.
6. Barrett T, Wilhite SE, Ledoux P, *et al.* NCBI GEO: archive for functional genomics data sets-update. *Nucleic Acids Res* 2013; 41: D991–D995.
7. Szklarczyk D, Morris JH, Cook H, *et al.* The STRING database in 2017: quality-controlled protein–protein association networks, made broadly accessible. *Nucleic Acids Res* 2017; 45: D362–D368.
8. Lamb J, Crawford ED, Peck D, *et al.* The Connectivity Map: using gene-expression signatures to connect small molecules, genes, and disease. *Science* 2006; 313: 1929–1935.
9. Lamb J, Ramaswamy S, Ford HL, *et al.* A mechanism of cyclin D1 action encoded in the patterns of gene expression in human cancer. *Cell* 2003; 114: 323–334.
10. Gerald KB. Nonparametric statistical methods. *Nurse Anesth* 1991; 2: 93–95.
11. Subramanian A, Narayan R, Corsello SM, *et al.* A next generation connectivity map: L1000 platform and the first 1,000,000 Profiles. *Cell* 2017; 171: 1437–1452 e1417.
12. Qu XA and Rajpal DK. Applications of Connectivity Map in drug discovery and development. *Drug Discov Today* 2012; 17: 1289–1298.
13. Wang Y, Arora K, Yang F, *et al.* PP-2, a src-kinase inhibitor, is a potential corrector for F508del-CFTR in cystic fibrosis. *bioRxiv* 2018:288324.
14. Sontake V, Wang Y, Kasam RK, *et al.* Hsp90 regulation of fibroblast activation in pulmonary fibrosis. *JCI Insight* 2017; 2: e91454.
15. Iorio F, Bosotti R, Scacheri E, *et al.* Discovery of drug mode of action and drug repositioning from transcriptional responses. *Proc Natl Acad Sci U S A* 2010; 107: 14621–14626.
16. Iorio F, Isacchi A, di Bernardo D and Brunetti-Pierri N. Identification of small molecules enhancing autophagic function from drug network analysis. *Autophagy* 2010; 6: 1204–1205.
17. Karatzas E, Bourdakou MM, Kolios G, *et al.* Drug repurposing in idiopathic pulmonary fibrosis filtered by a bioinformatics-derived composite score. *Sci Rep* 2017; 7: 12569.
18. Peyvandipour A, Saberian N, Shafi A, *et al.* A novel computational approach for drug repurposing using systems biology. *Bioinformatics* 2018; 34: 2817–2825.
19. Saito S, Zhuang Y, Suzuki T, *et al.* HDAC8 inhibition ameliorates pulmonary fibrosis. *Am J Physiol Lung Cell Mol Physiol* 2019; 316: L175–L186.
20. Sanders YY, Hagood JS, Liu H, *et al.* Histone deacetylase inhibition promotes fibroblast apoptosis and ameliorates pulmonary fibrosis in mice. *Eur Respir J* 2014; 43: 1448–1458.

21. Mukherjee S, Ayaub EA, Murphy J, *et al.* Disruption of calcium signaling in fibroblasts and attenuation of bleomycin-induced fibrosis by nifedipine. *Am J Respir Cell Mol Biol* 2015; 53: 450–458.

22. Tanaka KI, Niino T, Ishihara T, *et al.* Protective and therapeutic effect of felodipine against bleomycin-induced pulmonary fibrosis in mice. *Sci Rep* 2017; 7: 3439.

23. Barrett T, Troup DB, Wilhite SE, *et al.* NCBI GEO: mining tens of millions of expression profiles-database and tools update. *Nucleic Acids Res* 2007; 35: D760–D765.

24. DePianto DJ, Chandriani S, Abbas AR, *et al.* Heterogeneous gene expression signatures correspond to distinct lung pathologies and biomarkers of disease severity in idiopathic pulmonary fibrosis. *Thorax* 2015; 70: 48–56.

25. Wang Y, Yella J, Chen J, *et al.* Unsupervised gene expression analyses identify IPF-severity correlated signatures, associated genes and biomarkers. *BMC Pulm Med* 2017; 17: 133.

26. Konishi K, Gibson KF, Lindell KO, *et al.* Gene expression profiles of acute exacerbations of idiopathic pulmonary fibrosis. *Am J Respir Crit Care Med* 2009; 180: 167–175.

27. Rosas IO, Richards TJ, Konishi K, *et al.* MMP1 and MMP7 as potential peripheral blood biomarkers in idiopathic pulmonary fibrosis. *PLoS Med* 2008; 5: e93.

28. Meltzer EB, Barry WT, D'Amico TA, *et al.* Bayesian probit regression model for the diagnosis of pulmonary fibrosis: proof-of-principle. *BMC Med Genomics* 2011; 4: 70.

29. Hsu E, Shi H, Jordan RM, *et al.* Lung tissues in patients with systemic sclerosis have gene expression patterns unique to pulmonary fibrosis and pulmonary hypertension. *Arthritis Rheum* 2011; 63: 783–794.

30. Horimasu Y, Ishikawa N, Taniwaki M, *et al.* Gene expression profiling of idiopathic interstitial pneumonias (IIPs): identification of potential diagnostic markers and therapeutic targets. *BMC Med Genet* 2017; 18: 88.

31. Ritchie ME, Phipson B, Wu D, *et al.* limma powers differential expression analyses for RNA-sequencing and microarray studies. *Nucleic Acids Res* 2015; 43: e47.

32. Carvalho-Silva D, Pierleoni A, Pignatelli M, *et al.* Open Targets Platform: new developments and updates two years on. *Nucleic Acids Res* 2018; 47: D1056–D1065.

33. Davis AP, Grondin CJ, Johnson RJ, *et al.* The comparative toxicogenomics database: update 2019. *Nucleic Acids Res* 2019; 47: D948–D954.

34. Yu W, Clyne M, Khoury MJ, *et al.* Phenopedia and Genopedia: disease-centered and gene-centered views of the evolving knowledge of human genetic associations. *Bioinformatics* 2010; 26: 145–146.

35. Stelzer G, Rosen N, Plaschkes I, *et al.* The GeneCards suite: from gene data mining to disease genome sequence analyses. *Curr Protoc Bioinformatics* 2016; 54: 1.30.31–31.30.33.

36. Chen J, Bardes EE, Aronow BJ, *et al.* ToppGene Suite for gene list enrichment analysis and candidate gene prioritization. *Nucleic Acids Res* 2009; 37: W305–W311.

37. Maher TM and Strek ME. Antifibrotic therapy for idiopathic pulmonary fibrosis: time to treat. *Respir Res* 2019; 20: 205.

38. Adams TS, Schupp JC, Poli S, *et al.* Single-cell RNA-seq reveals ectopic and aberrant lung-resident cell populations in idiopathic pulmonary fibrosis. *Sci Adv* 2020; 6: eaba1983.

39. Habermann AC, Gutierrez AJ, Bui LT, *et al.* Single-cell RNA sequencing reveals profibrotic roles of distinct epithelial and mesenchymal lineages in pulmonary fibrosis. *Sci Adv* 2020; 6: eaba1972.

40. Reyfman PA, Walter JM, Joshi N, *et al.* Single-cell transcriptomic analysis of human lung provides insights into the pathobiology of pulmonary fibrosis. *Am J Respir Crit Care Med* 2019; 199: 1517–1536.

41. Jiang A and Jegga AG. Characterizing drug-related adverse events by joint analysis of biomedical and genomic data: a case study of drug-induced pulmonary fibrosis. *AMIA Jt Summits Transl Sci Proc* 2018; 2017: 91–97.

42. Costello JC, Heiser LM, Georgii E, *et al.* A community effort to assess and improve drug sensitivity prediction algorithms. *Nat Biotechnol* 2014; 32: 1202–1212.

43. Kasam RK, Ghandikota S, Soundararajan D, *et al.* Inhibition of Aurora Kinase B attenuates fibroblast activation and pulmonary fibrosis. *EMBO Mol Med* 2020: e12131.

44. Wollin L, Wex E, Pautsch A, *et al.* Mode of action of nintedanib in the treatment of idiopathic pulmonary fibrosis. *Eur Respir J* 2015; 45: 1434–1445.

45. Huang X, Wang W, Yuan H, *et al.* Sunitinib, a small-molecule kinase inhibitor, attenuates

bleomycin-induced pulmonary fibrosis in mice. *Tohoku J Exp Med* 2016; 239: 251–261.

46. Raghu G, Behr J, Brown KK, *et al.*; ARTEMIS-IPF Investigators*. Treatment of idiopathic pulmonary fibrosis with ambrisentan: a parallel, randomized trial. *Ann Intern Med* 2013; 158: 641–649.
47. Vallath S, Hynds RE, Succony L, *et al.* Targeting EGFR signalling in chronic lung disease: therapeutic challenges and opportunities. *Eur Respir J* 2014; 44: 513–522.
48. Epstein Shochet G, Brook E, Eyal O, *et al.* Epidermal growth factor receptor paracrine upregulation in idiopathic pulmonary fibrosis fibroblasts is blocked by nintedanib. *Am J Physiol Lung Cell Mol Physiol* 2019; 316: L1025–L1034.
49. Genovese T, Mazzon E, Di Paola R, Muià C, *et al.* Role of endogenous and exogenous ligands for the peroxisome proliferator-activated receptor alpha in the development of bleomycin-induced lung injury. *Shock* 2005; 24: 547–555.
50. Janssen LJ, Mukherjee S and Ask K. Calcium homeostasis and ionic mechanisms in pulmonary fibroblasts. *Am J Respir Cell Mol Biol* 2015; 53: 135–148.
51. Han AC, Deng JX, Huang QS, *et al.* Verapamil inhibits scar formation after peripheral nerve repair in vivo. *Neural Regen Res* 2016; 11: 508–511.
52. Kolb M, Raghu G, Wells AU, *et al.*; INSTAGE Investigators. Nintedanib plus sildenafil in patients with idiopathic pulmonary fibrosis. *N Engl J Med* 2018; 379: 1722–1731.
53. Behr J, Kolb M, Song JW, *et al.* Nintedanib and sildenafil in patients with idiopathic pulmonary fibrosis and right heart dysfunction. A prespecified subgroup analysis of a double-blind randomized clinical trial (INSTAGE). *Am J Respir Crit Care Med* 2019; 200: 1505–1512.